Signal Transduction:

Targeting CB_2-GPR55 Receptor Heteromers Modulates Cancer Cell Signaling

Estefanía Moreno, Clara Andradas, Mireia Medrano, María M. Caffarel, Eduardo Pérez-Gómez, Sandra Blasco-Benito, María Gómez-Cañas, M. Ruth Pazos, Andrew J. Irving, Carme Lluís, Enric I. Canela, Javier Fernández-Ruiz, Manuel Guzmán, Peter J. McCormick and Cristina Sánchez

J. Biol. Chem. *published online June 18, 2014*

Access the most updated version of this article at doi: 10.1074/jbc.M114.561761

Find articles, minireviews, Reflections and Classics on similar topics on the JBC Affinity Sites.

Alerts:
- When this article is cited
- When a correction for this article is posted

Click here to choose from all of JBC's e-mail alerts

This article cites 0 references, 0 of which can be accessed free at
http://www.jbc.org/content/early/2014/06/18/jbc.M114.561761.full.html#ref-list-1

Downloaded from http://www.jbc.org/ by guest on July 18, 2014

JBC Papers in Press. Published on June 18, 2014 as Manuscript M114.561761
The latest version is at http://www.jbc.org/cgi/doi/10.1074/jbc.M114.561761

Targeting CB_2-GPR55 receptor heteromers modulates cancer cell signaling*

Estefanía Moreno[1,2,3,†], Clara Andradas[4,5,†], Mireia Medrano[1,2,3,†], María M. Caffarel[4,6], Eduardo Pérez-Gómez[4,5], Sandra Blasco-Benito[4,5], María Gómez-Cañas[7,2,8], M Ruth Pazos[7,2], Andrew J. Irving[9], Carme Lluís[1,2,3], Enric I. Canela[1,2,3], Javier Fernández-Ruiz[7,2,8], Manuel Guzmán[2,4,8], Peter J. McCormick[1,2,3,10*], Cristina Sánchez[4,5*]

[1]Dept. Biochemistry and Molecular Biology, University of Barcelona, 08028 Barcelona, Spain

[2]Centro de Investigación Biomédica en Red de Enfermedades Neurodegenerativas (CIBERNED), 28031 Madrid, Spain

[3]Institute of Biomedicine of the University of Barcelona, 08028 Barcelona, Spain

[4]Dept. Biochemistry and Molecular Biology I, School of Biology / Instituto Universitario de Investigación en Neuroquímica, School of Medicine, Complutense University, 28040 Madrid, Spain

[5]Instituto de Investigación Hospital 12 de Octubre, 28041 Madrid, Spain

[6]Present address: Dept. Pathology, University of Cambridge, CB2 1QP Cambridge, UK

[7]Dept. Biochemistry and Molecular Biology III / Instituto Universitario de Investigación en Neuroquímica, School of Medicine, Complutense University, 28040 Madrid, Spain

[8]Instituto Ramón y Cajal de Investigación Sanitaria (IRYCIS)

[9]Division of Neuroscience, Ninewells Hospital, University of Dundee, DD1 9SY Dundee, UK

[10]School of Pharmacy, University of East Anglia, Norwich Research Park, NR4 7TJ Norwich, UK

[†]These authors contributed equally to the work

*These authors co-directed the work

Running title**:** *CB_2R-GPR55 heteromers in cancer cells*

To whom correspondence should be addressed: Cristina Sánchez, Department of Biochemistry and Molecular Biology I, School of Biology, Complutense University, C/ José Antonio Novais, 2, 28040 Madrid, Spain, Tel.: (+34) 913944668; Fax: (+34) 913944672; E-mail: cristina.sanchez@quim.ucm.es; Peter J. McCormick, School of Pharmacy, CP 1.44, University of East Anglia, Norwich Research Park, Norwich NR4 7TJ, United Kingdom, (+44) (0) 1603 597197; E-mail: p.mccormick@uea.ac.uk

Keywords: cannabinoids; cannabinoid receptors; cancer; GPCR; Signal transduction; CB_2 receptor; GPR55; receptor heteromers

Downloaded from http://www.jbc.org/ by guest on July 18, 2014

Copyright 2014 by The American Society for Biochemistry and Molecular Biology, Inc.

Background: Cannabinoid receptor CB_2 (CB_2R) and GPR55 are overexpressed in cancer cells and control cell fate.
Results: CB_2R and GPR55 form heteromers in cancer cells which impact signaling of each protomer.
Conclusion: CB_2R-GPR55 heteromers drive biphasic signaling responses as opposed to the individual receptors via cross-antagonism.
Significance: These heteromers may explain some of the biphasic effects of cannabinoids and thus constitute potential new targets in oncology.

ABSTRACT

The G protein-coupled receptors CB_2 (CB_2R) and GPR55 are overexpressed in cancer cells and human tumors. As a modulation of GPR55 activity by cannabinoids has been suggested, we analyzed whether this receptor participates in cannabinoid effects on cancer cells. Here, we show that CB_2R and GPR55 form heteromers in cancer cells, that these structures possess unique signaling properties, and that modulation of these heteromers can modify the antitumoral activity of cannabinoids *in vivo*. These findings unveil the existence of previously unknown signaling platforms that help explain the complex behavior of cannabinoids and may constitute new targets for therapeutic intervention in oncology.

G protein-coupled receptors (GPCR) participate in the control of many different physiological processes and their de-regulation contributes to numerous human diseases (1,2). Two decades ago, cannabinoid receptor type 1 (CB_1R) and type 2 (CB_2R) were identified and cloned (3). They are part of the endocannabinoid system, which consists at least of these two receptors, their endogenous ligands (the endocannabinoids) and the enzymes that produce and metabolize these signaling lipids (3). This system modulates a wide variety of physiological functions, including cell fate (3,4). Thus, it has been described that cannabinoids, in most cases via CB_1R and/or CB_2R, direct cells towards proliferation, differentiation or death depending on the cell type and its specific context (5). In tumor cells in particular, these compounds usually produce proliferation-inhibiting and death-inducing effects both *in vitro* and *in vivo* (6), making them promising therapeutic options for the management of cancer. More recently, another GPCR, G protein-coupled receptor 55 (GPR55), has been related to cannabinoids (7). In this case, the pharmacology of the receptor is quite controversial and, although some authors have reported cannabinoid actions via GPR55, to date this receptor does not formally belong to the cannabinoid receptor family (8). Several publications support that lysophosphatidylinositol (LPI), another signaling lipid, is a putative GPR55 endogenous ligand (9,10). Like its close relatives CB_1R and CB_2R, GPR55 has been implicated in the control of cancer cell fate (11). Specifically, this receptor promotes cancer cell proliferation both in cell cultures and in animal models of cancer (12-14). However, the mechanistic details behind these effects remain unclear, in part due to the lack of clarity on the receptor's pharmacology.

The classical pharmacological paradigm associating one ligand with one receptor, and one receptor with one signaling pathway is being replaced with the view that GPCR receptor-receptor interactions are an important mechanism that can modulate each protomer's pharmacological properties (15). Here, we aimed at determining whether CB_2R and GPR55, two receptors that are overexpressed in most human tumors and control cancer cell fate (6,12,13), can form heteromers in cancer cells and, if so, whether these complexes might play a role in cannabinoid signaling in tumors.

EXPERIMENTAL PROCEDURES

Cells, cell cultures and transfections - HEK293 AD cells stably expressing CB_2R (HEK-CB_2), HA-GPR55 (HEK-GPR55) or co-expressing both receptors (HEK-CB_2-GPR55) were developed as previously described (16,17). All HEK293-derived cells were grown in DMEM (Gibco, Paisley, Scotland, UK) supplemented with 2 mM L-glutamine, 100 µg/mL sodium pyruvate, 100 U/mL penicillin/streptomycin, MEM Non-Essential Amino Acids Solution (1/100), and 10% (v/v) heat inactivated FBS (Invitrogen, Paisley, Scotland, UK) in the presence of the

Downloaded from http://www.jbc.org/ by guest on July 18, 2014

corresponding selection antibiotics (0.2 mg/mL of zeocin for HEK-CB_2 cells, 0.3 mg/mL of G418 for HEK-GPR55 cells or 0.2 mg/mL of zeocin and 0.3 mg/mL of G418 for HEK-CB_2-GPR55 cells). BT474 human breast adenocarcinoma cells endogenously expressing CB_2R and GPR55 (authors' unpublished real-time quantitative PCR data), or stably transfected with a 3xHA-GPR55 construct (BT474-GPR55) and selected by FACS, were maintained in RPMI supplemented with 10% FBS, penicillin/streptomycin and 0.4 mg/mL G418. Human glioblastoma T98G cells endogenously expressing CB_2R and GPR55 (at similar levels than BT474 cells, authors' unpublished real-time quantitative PCR data) or stably transfected with selective CB_2R or GPR55 shRNAs (Genecopoeia, Rockville, MD, US) and selected by FACS, were grown in DMEM supplemented with 2 mM L-glutamine, 100 µg/mL sodium pyruvate, 100 U/mL penicillin/streptomycin, MEM Non-Essential Amino Acids Solution (1/100), and 10% (v/v) heat inactivated FBS in the presence of the corresponding selection antibiotic (5 g/mL puromicin for T98G-shGPR55 and T98G-shCB_2). For transient transfections, HEK293 and BT474 cells were transfected with the corresponding fusion protein cDNA by the PEI (PolyEthylenImine, Sigma, St. Louis, MO, USA) method (18).

Bioluminescence Resonance Energy Transfer (BRET) - For BRET, GPR55-Rluc, CB_2R-YFP and Ghrelin 1a receptor-YFP fusion proteins were obtained as follows: the human cDNAs for CB_2R, GPR55 or Ghrelin 1a receptor were cloned into pcDNA3.1, and were amplified without their stop codons using sense and antisense primers harbouring unique EcoRI and BamHI sites for CB_2R or ghrelin receptor, or harbouring Hind III and BamHI for GPR55. The amplified fragments were subcloned to be in-frame with *Renilla Luciferase* (Rluc) into the EcoRI and BamHI restriction sites of pcDNA3.1-RLuc vector (p*RLuc*-N1; PerkinElmer, Wellesley, MA) or pEYFP-N1 vector (enhanced yellow variant of GFP; Clontech, Heidelberg, Germany) to generate the plasmids that express proteins fused to RLuc or YFP on the C-terminal end (GPR55-RLuc, CB_2R-YFP and Ghrelin 1a receptor-YFP). Expression of constructs was tested as previously described (19). HEK293 or BT474 cells were transiently co-transfected with a constant amount of cDNA encoding for proteins fused to Rluc as a BRET donor, and with increasing amounts of the cDNA corresponding to proteins fused to YFP as a BRET acceptor. The fusion protein expression and BRET values were quantified as previously described (20) using a Mithras LB 940 that allows the integration of the signals detected in the short-wavelength filter at 485 nm (440-500 nm) and the long-wavelength filter at 530 nm (510-590 nm) (20). The net BRET is defined as [(long-wavelength emission)/(short-wavelength emission)]-Cf where Cf corresponds to [(long-wavelength emission)/(short-wavelength emission)] for the donor construct expressed alone in the same experiment. Data were fitted to a non-linear regression equation, assuming a single phase saturation curve with GraphPad Prism software (San Diego, CA, USA). BRET is expressed as miliBRET units, mBU (net BRET x 1000). In saturation curves, the relative amount of BRET is given as a function of 100 x the ratio between the fluorescence of the acceptor (YFP) and the luciferase activity of the donor (Rluc).

In Situ Proximity Ligation Assays (PLA) - Cells were grown on glass coverslips and were fixed in 4% paraformaldehyde, washed with PBS containing 20 mM glycine, permeabilized with the same buffer containing 0.05% Triton X-100 and successively washed with PBS. CB_2R-GPR55 heteromers were detected using the Duolink II *in situ* PLA detection Kit (OLink; Bioscience, Uppsala, Sweden). After 1 h incubation at 37ºC with the blocking solution in a preheated humidity chamber, cells were incubated overnight in the antibody dilution medium with a mixture of equal amounts of mouse anti-HA antibody (1:100, Sigma) or rabbit anti GPR55 antibody (1:100, Abcam, Cambridge, UK) directly coupled to a DNA minus chain to detect HA-GPR55 or endogenous GPR55, and rabbit anti-CB_2R antibody (1:100, Cayman Chemical, Ann Arbor, MI) directly coupled to a DNA plus chain. Cells were washed with wash buffer A at room temperature and were incubated in a pre-heated humidity chamber for 30 min at 37ºC, with the ligation solution (Duolink II Ligation stock 1:5

Downloaded from http://www.jbc.org/ by guest on July 18, 2014

and Duolink II Ligase 1:40) to induce annealing and ligation of the two DNA probes. Amplification was done with the Duolink II Detection Reagents Red Kit, that contains fluorescence nucleotides. After exhaustively washing at room temperature with wash buffer B, cells were mounted using the mounting medium with DAPI. The samples were observed in a Leica SP2 confocal microscope (Leica Microsystems, Mannheim, Germany). Red fluorescent images were processed with Image J software. PLA requires that both receptors be close enough to allow the two different antibody-DNA probes to be able to ligate (<17nm) (21,22). If the receptors are within sufficient proximity, a punctate fluorescent signal can be detected by confocal microscopy.

Dynamic mass redistribution (DMR) assays - The agonist-induced cell global signaling signature was determined by a label-free technology measuring the Dynamic mass redistribution (DMR) using an EnSpire® Multimode Plate Reader (PerkinElmer, Waltham, MA, USA) (23). Refractive waveguide grating optical biosensors, integrated in 384-well microplates, allow measurements of changes in local optical density in a detection zone up to 150 nm above the surface of the sensor. Cellular mass movements induced upon receptor activation were detected by illuminating the underside of the biosensor with polychromatic light and measured as changes in wavelength of the reflected monochromatic light that is a function of the index of refraction. The magnitude of this wavelength shift (in picometers) is directly proportional to the amount of cell movement. Briefly, 24 h before the assay, cells (10,000/well) were seeded in 384-well sensor microplates and cultured to obtain 70-80% confluent monolayers. Previous to the assay, cells were washed twice with assay buffer (HBSS with 20 mM HEPES, pH 7.15) and incubated for 2 h in assay-buffer with 0.1% DMSO in the reader at 24°C. Hereafter, the sensor plate was scanned and a baseline optical signature was recorded before adding the test compounds dissolved in assay buffer containing 0.1% DMSO. DMR responses were monitored for at least 2000 s. Kinetic results were analyzed using the EnSpire Workstation Software v 4.10.

cAMP production - Homogeneous time-resolved fluorescence energy transfer (HTRF) assays were performed using the Lance Ultra cAMP kit (PerkinElmer, Waltham, MA, USA), based on competitive displacement of a europium chelate-labelled cAMP tracer bound to a specific antibody conjugated to acceptor beads. We first established the optimal cell density for an appropriate fluorescent signal. This was done by measuring the TR-FRET signal determined as a function of forskolin concentration using different cell densities. The forskolin dose-response curves were related to the cAMP standard curve in order to establish which cell density provides a response that covers most of the dynamic range of cAMP standard curve. Cells (1000 /well) were pre-treated with the antagonists or the corresponding vehicle (DMSO) in white ProxiPlate 384-well microplates (PerkinElmer) at 25°C for 20 min, and stimulated with agonists for 15 min before adding 0.5 µM forskolin or vehicle, and incubating for an additional 15 min period. Fluorescence at 665 nm was analyzed on a PHERAstar Flagship microplate reader equipped with a HTRF optical module (BMG Lab technologies, Offenburg, Germany).

ERK-1/2 phosphorylation - Cells (35,000/well) seeded in 96 wells Poly-D-Lysine Coated plates (Sigma-Aldrich), were pre-treated at 25°C for 20 min with the antagonists and stimulated for an additional 7 min with the indicated agonists. Phosphorylation was determined in white ProxiPlate 384-well microplates (PerkinElmer) by alpha-screen bead-based technology using the Amplified Luminiscent Proximity Homogeneous Assay kit (PerkinElmer, Waltham, MA, USA) and the Enspire Multimode Plate Reader (PerkinElmer). Phosphorylation is expressed in arbitrary units, ALPHA counts, as measured by light emission at 520-620 nm by the acceptor beads. To evaluate phospho-ERK-1/2 expression in tumors, a Western blot analysis was performed. Tumor lysates were subjected to SDS-PAGE, and proteins transferred onto polyvinylidene fluoride membranes. Blots were incubated with anti-phospho-ERK (Thr202/Tyr204), anti-ERK (Cell Signaling Technology, Danvers, MA) and anti-α-tubulin (Sigma-Aldrich) antibodies. Luminograms were obtained with the Amersham Enhanced

Downloaded from http://www.jbc.org/ by guest on July 18, 2014

Chemiluminescence Detection Kit (GE Healthcare, Uppsala, Sweden), and the densitometric analysis was performed with Quantity One software (Bio-Rad, Hercules, CA).

[^{35}S]GTPγS binding assays – HEK-GPR55 cells were rinsed twice in phosphate-buffered saline, detached from dishes by incubation with a buffer containing 5.6 mM glucose, 5 mM KCl, 5 mM HEPES, 137 mM NaCl, 1 mM EGTA, pH 7.4, and collected by centrifugation (500g) at 4ºC. The pellets were then resuspended in ice-cold lysis buffer (0.2 mM $MgSO_4$, 0.38 mM KH_2PO_4, 0.61 mM Na_2HPO_4, 0.5% PMSF, pH 7.4) and homogenized by vortexing. HEK-GPR55 membranes were isolated by centrifugation (20,000g for 20 min) and pellets were resuspended in 50 mM Tris-HCl buffer, pH 7.4. Protein concentration was determined by DCTM Protein Assay Kit (Bio-Rad, Madrid, Spain). Membranes were stored at -80ºC until used for analysis of LPI-induced stimulation of [^{35}S]GTPγS binding. For this analysis, we followed a previously-published procedure (24), in which cell membranes (20 μg protein/mL) were incubated for 120 min at 30°C in assay buffer (100 mM NaCl, 50 mM Tris-HCl, 10 mM $MgCl_2$, 1 mM EGTA, 1 mM DTT, 50 μM GDP, and 1 mg/mL BSA, pH 7.4) containing 0.1 nM [^{35}S]GTPγS and increasing concentrations of LPI (10^{-10}–10^{-5} M) in the presence or the absence of 10^{-6} M of Δ^9-tetrahydrocannabinol (THC, The Health Concept, Richelbach, Germany). Nonspecific binding was determined in the presence of 10 μM unlabeled GTPγS. Reactions were terminated by rapid filtration performed by a Harvester filtermate (PerkinElmer, Madrid, Spain) with Filtermat A GF/C filters. Filters were rinsed nine times with washing buffer (50mM Tris-HCl and 1 mg/mL BSA, pH 7.4) and left to dry, and melt-on scintillation pads (Meltilex A, Perkin Elmer) were melted onto them. The bound radioactivity was quantified by liquid scintillation spectrophotometer (Wallac MicroBeta Trilux, PerkinElmer). Results were normalized as % change over basal level (set at 100%) and corresponded to three separate experiments, each performed in triplicate. Data were analyzed by nonlinear regression analysis of sigmoidal dose-response curves using GraphPad Prism 5.01 (GraphPad, San Diego, CA).

Tumour generation and animal treatments - Tumors (n=6/experimental group) were induced in 6-week-old athymic male mice (Harlan Interfauna Iberica, Barcelona, Spain) by subcutaneous injection of $10x10^6$ T98G human glioblastoma cells in PBS supplemented with 0.1% glucose. Half of the animals were treated with double-stranded RNA duplexes for human GPR55 (ON-TARGETplus SMART pools) from Dharmacon-Thermo Scientific (Lafayette Colorado). Sequences were 5'-GAAUUCCGCAUGAACAUCAUU-3', 5'-GAGAAACAGCUUUAUCGUAUU-3', 5'-AAGAACAGGUGGCCCGAUUUU-3' and 5'-GCUACUACUUUGUCAUCAAUU-3'). The other half was treated with a non-targeted control siRNA from Applied Biosystems-Ambion (Austin, TX). The sequence was 5'-UUCUCCGAACGUGUCACGUtt-3'. siRNA was mixed with AteloGene (Koken, Tokyo, Japan) and was injected locally when tumours reached ca 200 mm^3 (day 1) and on day 7. At the same time, each group was daily treated peritumorally with 1.5 or 15 mg/Kg per day of THC (The Health Concept, Richelbach, Germany) or the corresponding vehicle (PBS supplemented with 5% BSA) for 15 days. Tumors were routinely measured with external caliper, and volume was calculated as $(4\pi/3) \times (\text{width}/2)^2 \times (\text{length}/2)$. At the end of the treatment, animals were sacrificed and tumors were collected.

RESULTS

Expression and functional characterization of CB_2R-GPR55 heteromers in transfected HEK293 cells - To analyze the possible molecular interaction between CB_2R and GPR55, Bioluminescence Resonance Energy Transfer (BRET) experiments were performed. HEK293 cells expressing a fixed amount of GPR55-Rluc as BRET donor and increasing amounts of CB_2R-YFP as BRET acceptor, generated a hyperbolic and saturable BRET signal (Fig. 1A) with a $BRET_{max}$ of 257±18 mBU and a $BRET_{50}$ of 7.3±1.2, that was not evident in cells expressing equivalent amounts of GPR55-Rluc and Ghrelin 1a receptor-YFP as negative control

Downloaded from http://www.jbc.org/ by guest on July 18, 2014

(Fig. 1A). These results support that CB_2R and GPR55 form heteromers in co-transfected cells.

We then analyzed whether the formation of these complexes alters the signaling properties of the individual protomers. To test which G-proteins are coupled to the receptors when expressed alone, we used a label-free approach that measures dynamic mass redistribution (DMR) in the bottom 150 nm of a cell monolayer through detection of changes in light diffraction (23). In HEK293 cells expressing CB_2R only (HEK-CB_2), the CB_2R-selective agonist HU-308 produced a robust DMR signal (Fig. 1B) that was sensitive to pertussis toxin (PTX) and not to cholera toxin (CTX) (Fig. 1C). This is in line with many previous reports showing coupling of CB_2R to Gi heterotrimeric proteins (3). In HEK293 cells expressing GPR55 only (HEK-GPR55), we observed that the GPR55 agonist LPI produced a strong response (Fig. 1D) that was insensitive to CTX or PTX treatment (Fig. 1E), suggestive of coupling to G proteins other than Gi and Gs, as previously reported (8). Importantly, neither LPI nor HU-308 showed any activity in non-transfected cells (Fig 1J), and both CB_2R and GPR55 agonists and antagonists showed selectivity for their respective receptors, with no agonist activation or antagonist blockade of the partner receptor in single-receptor expressing cells (Fig. 1B, D). Interestingly, in HEK293 cells overexpressing both receptors (HEK-CB_2-GPR55) we observed a similar coupling to G proteins but a different pharmacological behavior. In these cells, LPI induced a robust DMR signal (Fig. 1F) that was insensitive to CTX or PTX treatment (Fig. 1H, I), suggesting again coupling to G proteins different than Gi and Gs, and HU-308 induced a signal (Fig. 1G) that was blocked by PTX but not by CTX (Fig. 1H, I), indicating a Gi coupling. Surprisingly, the signal induced by LPI was completely blocked by the CB_2R antagonist AM630 (Fig. 1F), and the signaling induced by HU-308 was blocked by the GPR55 antagonist HMOPP benzoic acid (HBA) (Fig. 1G). This cross-antagonism phenomenon suggests that, through the heteromer, one receptor can be targeted by using the partner receptor antagonist.

Since DMR experiments are indicative of global receptor signaling, we next investigated heteromer function in specific signaling pathways. In HEK-CB_2 cells, HU-308 (Fig. 2A) but not LPI (Fig. 2B) prevented the increase in cAMP levels elicited by forskolin (FK), an effect that was blocked by PTX and not by CTX (Fig. 2A), and by AM630 and not by HBA (Fig. 2C). In HEK-GPR55 cells, LPI produced no effect on FK-induced cAMP levels (Fig. 2D), supporting coupling of this receptor to G proteins different than Gi or Gs. HU-308 did not induce any effect in these cells either (Fig. 2E). As observed in the label-free assays, HEK-CB_2-GPR55 cells showed a different pharmacological behavior. HU-308 alone was still able to block the FK-induced cAMP increase through a PTX-sensitive mechanism (Fig. 1F). As expected in these cells, LPI was not able to increase or decrease (Fig. 1G) FK-stimulated cAMP levels. However, simultaneous activation of CB_2R and GPR55 prevented HU-308 action (Fig. 1G), which is indicative of a negative cross-talk between both receptors. Moreover, in HEK-CB_2-GPR55 cells, HU-308 effects on cAMP levels were blocked not only by AM630 but also by HBA (Fig. 1G). Similar negative cross-talk and cross-antagonism were detected in ERK-1/2 signaling. When expressed alone, activation of each receptor by its selective ligand resulted in a time- and dose-dependent increase in ERK-1/2 phosphorylation (Fig. 3A,B). In cells simultaneously expressing both receptors, activation of any of the protomers individually produced a similar response (Fig. 3C, D). However, co-activation of both receptors resulted in a reduced ERK-1/2 phosphorylation (Fig. 3E). In addition, LPI-induced ERK-1/2 phosphorylation was prevented by the CB_2R antagonist, and HU-308 action was blocked by the GPR55 antagonist (i.e. cross-antagonist) (Fig. 3E). Together, these results support that CB_2R and GPR55 form heteromers in co-transfected cells, and that, via these complexes, agonists and antagonists of one receptor are able to impair the signaling of the partner receptor.

Expression and functional characterization of CB_2R-GPR55 heteromers in human breast cancer cells - Next, we sought to determine whether CB_2R-GPR55 heteromers are present in a more physiological setting, i.e., human cancer cells. First, BRET saturation curves

Downloaded from http://www.jbc.org/ by guest on July 18, 2014

performed in human breast adenocarcinoma BT474 cells transfected to express GPR55-Rluc and increasing amounts of CB_2R-YFP indicated that these receptors also interact in cancer cells (Fig. 4A). This interaction was further confirmed by proximity ligation assays (PLA) in BT474 cells endogenously expressing CB_2R and stably expressing HA-GPR55 (BT474-GPR55). Heteromers were readily detectable in these cells (Fig. 4B, left panel) but not in cells not expressing CB_2R or upon removal of one of the primary antibodies (Fig. 4B, small panels). Of interest, the PLA-positive BT474 cells showed the same signaling profile as the aforementioned HEK-CB_2-GPR55 cells. Thus, in label-free experiments, HU-308 induced a DMR signal that was sensitive to PTX and not to CTX, LPI induced a signal that was insensitive to toxins, and both LPI and HU308 induced signals were blocked by the antagonist of the partner receptor (Fig. 4C-E). In addition, HU-308 (and not LPI) blocked FK-induced cAMP increase (Fig. 5A), an effect that was sensitive to PTX and not to CTX (Fig. 5B). The HU308-induced effect was also prevented by co-activation with LPI (negative cross-talk), and not only by a CB_2R antagonist but also by a GPR55 antagonist (cross-antagonism) (Fig. 5A). The negative cross-talk and cross-antagonism were also observed in the activation of ERK-1/2 (Fig. 5C-E). Collectively, these findings support the existence of CB_2R-GPR55 heteromers in cancer cells and show that these macromolecular structures have specific signaling properties.

Differential effects of THC in HEK293 cells expressing CB_2R-GPR55 heteromers or the single receptors - Next, we analyzed the signaling response of HEK293 and cancer cells to the cannabinoid agonist Δ^9-tetrahydrocannabinol (THC). In agreement with previous observations (3), THC dose-dependently reduced FK-increased cAMP levels (Fig. 6A) and enhanced ERK-1/2 phosphorylation (Fig. 6B) in HEK-CB_2 cells. Interestingly, in HEK-CB_2-GPR55 cells, a biphasic response was observed in both readouts. Thus, while low concentrations of THC decreased FK-induced cAMP, higher THC concentrations attenuated this effect (Fig. 6C). Analogously, low concentrations of THC increased ERK-1/2 phosphorylation, while higher concentrations reduced this response (Fig. 6D). In support of the notion that these two-phase effects of THC are distinctive of the heteromers, we observed that the U-shaped curve in the cAMP assays (Fig. 6E) and the bell-shaped curve in the ERK-1/2 activation data (Fig. 6F) became flattened when cells were pre-treated with either a CB_2R or a GPR55 antagonist. From these observations, we hypothesize the following mechanistic explanation for the biphasic action of THC (Fig. 6G): at low concentrations, THC (a well-reported CB_2R agonist) signals through CB_2R, thus producing a conceivable activation of ERK-1/2 and inhibition of FK-induced cAMP increase (Fig. 6G, upper panel). At higher concentrations, THC is able to target GPR55, thus acting as a receptor antagonist, as previously suggested in (25), and exerting a cross-antagonism over CB_2R through the heteromer, which would result in an attenuation of the CB_2R-mediated effects on ERK-1/2 activation and cAMP production (Fig. 6G, lower panel). In support of this idea, THC (that was not able to induce either DMR signals or ERK-1/2 phosphorylation in cells only expressing GPR55) decreased LPI-induced DMR responses (Fig. 6H) and ERK-1/2 activation (Fig. 6I) in HEK-GPR55 cells. The capability of THC to prevent LPI-induced activation of GPR55 was further confirmed by GTPγS binding assays. Thus, LPI produced a marked increase in [^{35}S]GTPγS binding in HEK-GPR55 membranes (E_{max} = 129±2 %; EC_{50} = 7.1±3.4 nM), an effect that was completely blocked by co-incubation with THC (Fig. 6J). Together, these results indicate that, at high concentrations, THC actually behaves as a GPR55 antagonist.

Involvement of CB_2R-GPR55 heteromers in the response of cancer cells to THC - We then went back to cancer cells to challenge this hypothesis. First, PLA experiments showed that neither low nor high THC concentrations disrupt the CB_2R-GPR55 heteromers (Fig. 7A). Second, as in HEK-CB_2-GPR55 cells, a two-phase effect of THC was observed in BT474-GPR55 cells on the modulation of both cAMP levels and ERK-1/2 phosphorylation, in which the response found at low concentrations was attenuated at higher concentrations (Fig. 7B). The U-shaped curve in

Downloaded from http://www.jbc.org/ by guest on July 18, 2014

the cAMP assays and the bell-shaped curve in the ERK-1/2 activation became less pronounced or even flattened when BT474-GPR55 cells were pre-treated with the GPR55 antagonist HBA (Fig. 7C) demonstrating that the antagonistic effect of THC on GPR55 modulates CB_2R signaling through CB_2R-GPR55 heteromers.

Our hypothesis was further corroborated in T98G cells, a human glioblastoma cell line that endogenously expresses both CB_2R (26) and GPR55 (12). By PLA, we detected red spots corresponding to CB_2R-GPR55 heteromers (Fig. 8A, left top panel). Treatment of cells with either low or high concentrations of THC did not alter this staining (Fig. 8A, top panels), suggesting that the heteromers are not disrupted by the cannabinoid. The CB_2R-GPR55 complexes were not detected in the negative controls in which one of the primary antibodies was omitted or in T98G cells in which CB_2R (T98G-shCB_2) or GPR55 (T98G-shGPR55) expression was silenced (Fig. 8A, bottom panels). As in transfected cells, a two-phase effect of THC was observed in T98G cells on the modulation of both cAMP levels and ERK-1/2 phosphorylation, in which the response found at low concentrations was attenuated at higher concentrations (Fig. 8B). Finally, we analyzed the strength of our hypothesis in an *in vivo* setting. Subcutaneous tumors were generated by injection of T98G cells into athymic male mice. Tumors increased their growth slightly in response to a low THC dose (although no statistical differences were observed), while a higher THC dose produced the opposite effect, i.e. a significant reduction in tumor growth (Fig. 8C). According to our hypothesis, the low-dose effect would be produced mainly via activation of CB_2R, and the high-dose effect via cross-antagonism of CB_2R upon targeting of GPR55. The direct antagonism of GPR55, a receptor that has been previously shown to drive tumorigenesis (12-14), by THC may contribute to this strong antitumoral response. Supporting the idea that GPR55 behaves as a tumor-growth brake when targeted by high doses of THC, we observed that GPR55-silenced tumors increased their growth when exposed to THC (Fig. 8C). The differential effects of THC on tumor growth occurred in concert with differential changes in the levels of activated ERK-1/2, i.e. a reduction when CB_2R and GPR55 were co-expressed and an enhancement when GPR55 was silenced (Fig. 8D, E). These results support our hypothesis and suggest that the well-established cannabinoid target CB_2R, as well as GPR55, co-participate in part via direct receptor-receptor interaction in the control of tumor growth in response to THC.

DISCUSSION

The findings reported in this study lead to three important conclusions regarding the role of cannabinoids and their cognate receptors. First, we demonstrate the existence and function of CB_2R-GPR55 heteromers in cancer cells. Second, we show that expression of these receptor heteromers has a major impact on cannabinoid signaling in these cells. Finally, our results suggest that direct targeting of CB_2R-GPR55 via appropriate doses of THC may be an effective approach to reducing tumor growth.

Receptor heteromers involving the sister cannabinoid receptor CB_1 have been the focus of intense research. Thus, CB_1R have been previously shown to interact with other GPCR, including dopamine D_2 receptors (which promotes a switch in the preferential coupling from Gi to Gs) (27), D_2 receptors and adenosine A_{2A} receptors simultaneously (producing a negative modulation of D_2 receptor function by A_{2A} and CB_1R agonists) (28), opioid receptors (which produces a negative crosstalk between protomers) (29), orexin OX_1 receptors (eliciting a positive crosstalk in response to orexin and cross-antagonism) (30) and angiotensin AT_1 receptors (resulting in the potentiation of AT_1 receptor signaling) (31). More recently, co-immunoprecipitation assays in HEK293 cells have suggested that CB_1R can form heteromers with GPR55 (32). In contrast to CB_1R, very little is known about the possible existence and functional relevance of heteromers involving CB_2R. A recent study has shown that CB_2R heteromerize with CB_1R in neuronal cells in culture and *in vivo* (19). In these systems, co-activation of both receptors results in a negative cross-talk and a bidirectional cross-antagonism (19). However, CB_2R signaling can be conceivably more relevant in non-differentiated cells, in which the receptor is highly abundant,

Downloaded from http://www.jbc.org/ by guest on July 18, 2014

than in terminally-differentiated cells such as neurons, in which the receptor is scarce (3,33). Specifically, CB_2R, as well as GPR55, are notably overexpressed in a wide variety of cancer cell lines and human malignant tumors (6,11), in which they play pivotal roles in controlling cancer cell fate (6,11-14). It is tempting to speculate that CB_2R-GPR55 heteromers may also exist and play pivotal signaling roles in other cells or tissues in which they are overexpressed, such as hematopoietic cells (16) or the bones (34).

More and more studies have attempted to address the physiological role of GPR55. This receptor has been implicated in cancer, where it is generally linked with growth and proliferation (12-14). However, the molecular and cellular mechanisms behind these effects are still unanswered. In addition, it has been unclear whether GPR55's effects on proliferation involve CB_2R or are independent. Considering the receptor heteromers discussed above and knowing that CB_2R and GPR55 have been functionally linked in hematopoietic cells (16), we pursued the hypothesis that CB_2R-GPR55 heteromers might play a role in GPR55's effects in cancer cells. Indeed, we found that these complexes were able to form in HEK293 cells and in both BT474 and T98G cancer cells, and that they display a cross-talk and cross-antagonism at the level of the cAMP and p-ERK-1/2 pathways. We also found different cell signaling effects at low and high concentrations of THC and that this bimodal effect required the presence of the heteromer. Our findings that THC appears to be an antagonist of GPR55, at least at the level of cell signaling both of the single receptor and within the CB_2R-GPR55 heteromer, were particularly surprising. Previous reports had indeed suggested as such (25), and the data we obtained in three different cell lines as well as in a mouse model of cancer *in vivo* support these conclusions. This is in line with the general idea that, despite the potential relationship between cannabinoid receptors and GPR55, their pharmacology is very different (8,35).

Finally, our discovery that CB_2R-GPR55 complexes have unique pharmacological and signaling properties and are critically involved in the response of cancer cells to THC both *in vitro* and *in vivo* opens new doors to the development of compounds targeting these heteromers as novel sites of intervention for future cancer studies. Our results also shed light on the possible molecular mechanisms underlying the well-known but still poorly understood biphasic effects of cannabinoids, which have been reported for several decades on their action on food intake, motor behavior or anxiety, among others (36-38).

Downloaded from http://www.jbc.org/ by guest on July 18, 2014

REFERENCES

1. Dorsam, R. T., and Gutkind, J. S. (2007) G-protein-coupled receptors and cancer. *Nat Rev Cancer* **7**, 79-94
2. Rosenbaum, D. M., Rasmussen, S. G., and Kobilka, B. K. (2009) The structure and function of G-protein-coupled receptors. *Nature* **459**, 356-363
3. Pertwee, R. G., Howlett, A. C., Abood, M. E., Alexander, S. P., Di Marzo, V., Elphick, M. R., Greasley, P. J., Hansen, H. S., Kunos, G., Mackie, K., Mechoulam, R., and Ross, R. A. (2010) International Union of Basic and Clinical Pharmacology. LXXIX. Cannabinoid receptors and their ligands: beyond CB and CB. *Pharmacol Rev* **62**, 588-631
4. Pacher, P., Batkai, S., and Kunos, G. (2006) The endocannabinoid system as an emerging target of pharmacotherapy. *Pharmacol Rev* **58**, 389-462
5. Guzman, M., Sanchez, C., and Galve-Roperh, I. (2002) Cannabinoids and cell fate. *Pharmacol Ther* **95**, 175-184
6. Velasco, G., Sanchez, C., and Guzman, M. (2012) Towards the use of cannabinoids as antitumour agents. *Nat Rev Cancer* **12**, 436-444
7. Brown, A. J. (2007) Novel cannabinoid receptors. *Br J Pharmacol* **152**, 567-575
8. Ross, R. A. (2009) The enigmatic pharmacology of GPR55. *Trends Pharmacol Sci* **30**, 156-163

9. Oka, S., Nakajima, K., Yamashita, A., Kishimoto, S., and Sugiura, T. (2007) Identification of GPR55 as a lysophosphatidylinositol receptor. *Biochem Biophys Res Commun* **362**, 928-934
10. Pertwee, R. G. (2010) Receptors and channels targeted by synthetic cannabinoid receptor agonists and antagonists. *Curr Med Chem* **17**, 1360-1381
11. Henstridge, C. M., Balenga, N. A., Kargl, J., Andradas, C., Brown, A. J., Irving, A., Sanchez, C., and Waldhoer, M. (2011) Minireview: recent developments in the physiology and pathology of the lysophosphatidylinositol-sensitive receptor GPR55. *Mol Endocrinol* **25**, 1835-1848
12. Andradas, C., Caffarel, M. M., Perez-Gomez, E., Salazar, M., Lorente, M., Velasco, G., Guzman, M., and Sanchez, C. (2011) The orphan G protein-coupled receptor GPR55 promotes cancer cell proliferation via ERK. *Oncogene* **30**, 245-252
13. Perez-Gomez, E., Andradas, C., Flores, J. M., Quintanilla, M., Paramio, J. M., Guzman, M., and Sanchez, C. (2013) The orphan receptor GPR55 drives skin carcinogenesis and is upregulated in human squamous cell carcinomas. *Oncogene* **32**, 2534-2542
14. Pineiro, R., Maffucci, T., and Falasca, M. (2011) The putative cannabinoid receptor GPR55 defines a novel autocrine loop in cancer cell proliferation. *Oncogene* **30**, 142-152
15. Rozenfeld, R., and Devi, L. A. (2010) Receptor heteromerization and drug discovery. *Trends Pharmacol Sci* **31**, 124-130
16. Balenga, N. A., Aflaki, E., Kargl, J., Platzer, W., Schroder, R., Blattermann, S., Kostenis, E., Brown, A. J., Heinemann, A., and Waldhoer, M. (2011) GPR55 regulates cannabinoid 2 receptor-mediated responses in human neutrophils. *Cell Res* **21**, 1452-1469
17. Henstridge, C. M., Balenga, N. A., Ford, L. A., Ross, R. A., Waldhoer, M., and Irving, A. J. (2009) The GPR55 ligand L-alpha-lysophosphatidylinositol promotes RhoA-dependent Ca2+ signaling and NFAT activation. *FASEB J* **23**, 183-193
18. Gonzalez, S., Rangel-Barajas, C., Peper, M., Lorenzo, R., Moreno, E., Ciruela, F., Borycz, J., Ortiz, J., Lluis, C., Franco, R., McCormick, P. J., Volkow, N. D., Rubinstein, M., Floran, B., and Ferre, S. (2012) Dopamine D4 receptor, but not the ADHD-associated D4.7 variant, forms functional heteromers with the dopamine D2S receptor in the brain. *Mol Psychiatry* **17**, 650-662
19. Callen, L., Moreno, E., Barroso-Chinea, P., Moreno-Delgado, D., Cortes, A., Mallol, J., Casado, V., Lanciego, J. L., Franco, R., Lluis, C., Canela, E. I., and McCormick, P. J. (2012) Cannabinoid receptors CB1 and CB2 form functional heteromers in brain. *J Biol Chem* **287**, 20851-20865
20. Carriba, P., Navarro, G., Ciruela, F., Ferre, S., Casado, V., Agnati, L., Cortes, A., Mallol, J., Fuxe, K., Canela, E. I., Lluis, C., and Franco, R. (2008) Detection of heteromerization of more than two proteins by sequential BRET-FRET. *Nat Methods* **5**, 727-733
21. Soderberg, O., Leuchowius, K. J., Gullberg, M., Jarvius, M., Weibrecht, I., Larsson, L. G., and Landegren, U. (2008) Characterizing proteins and their interactions in cells and tissues using the in situ proximity ligation assay. *Methods* **45**, 227-232
22. Trifilieff, P., Rives, M. L., Urizar, E., Piskorowski, R. A., Vishwasrao, H. D., Castrillon, J., Schmauss, C., Slattman, M., Gullberg, M., and Javitch, J. A. (2011) Detection of antigen interactions ex vivo by proximity ligation assay: endogenous dopamine D2-adenosine A2A receptor complexes in the striatum. *Biotechniques* **51**, 111-118
23. Schroder, R., Janssen, N., Schmidt, J., Kebig, A., Merten, N., Hennen, S., Muller, A., Blattermann, S., Mohr-Andra, M., Zahn, S., Wenzel, J., Smith, N. J., Gomeza, J., Drewke, C., Milligan, G., Mohr, K., and Kostenis, E. (2010) Deconvolution of complex G protein-coupled receptor signaling in live cells using dynamic mass redistribution measurements. *Nat Biotechnol* **28**, 943-949
24. Mato, S., Vidal, R., Castro, E., Diaz, A., Pazos, A., and Valdizan, E. M. (2010) Long-term fluoxetine treatment modulates cannabinoid type 1 receptor-mediated inhibition of adenylyl cyclase in the rat prefrontal cortex through 5-hydroxytryptamine 1A receptor-dependent mechanisms. *Mol Pharmacol* **77**, 424-434

Downloaded from http://www.jbc.org/ by guest on July 18, 2014

25. Anavi-Goffer, S., Baillie, G., Irving, A. J., Gertsch, J., Greig, I. R., Pertwee, R. G., and Ross, R. A. (2012) Modulation of L-alpha-lysophosphatidylinositol/GPR55 mitogen-activated protein kinase (MAPK) signaling by cannabinoids. *J Biol Chem* **287**, 91-104
26. Lorente, M., Torres, S., Salazar, M., Carracedo, A., Hernandez-Tiedra, S., Rodriguez-Fornes, F., Garcia-Taboada, E., Melendez, B., Mollejo, M., Campos-Martin, Y., Lakatosh, S. A., Barcia, J., Guzman, M., and Velasco, G. (2011) Stimulation of the midkine/ALK axis renders glioma cells resistant to cannabinoid antitumoral action. *Cell Death Differ* **18**, 959-973
27. Marcellino, S., Attar, H., Lievremont, D., Lett, M. C., Barbier, F., and Lagarde, F. (2008) Heat-treated Saccharomyces cerevisiae for antimony speciation and antimony(III) preconcentration in water samples. *Anal Chim Acta* **629**, 73-83
28. Navarro, G., Ferre, S., Cordomi, A., Moreno, E., Mallol, J., Casado, V., Cortes, A., Hoffmann, H., Ortiz, J., Canela, E. I., Lluis, C., Pardo, L., Franco, R., and Woods, A. S. (2010) Interactions between intracellular domains as key determinants of the quaternary structure and function of receptor heteromers. *J Biol Chem* **285**, 27346-27359
29. Rios, C., Gomes, I., and Devi, L. A. (2006) mu opioid and CB1 cannabinoid receptor interactions: reciprocal inhibition of receptor signaling and neuritogenesis. *Br J Pharmacol* **148**, 387-395
30. Ellis, J., Pediani, J. D., Canals, M., Milasta, S., and Milligan, G. (2006) Orexin-1 receptor-cannabinoid CB1 receptor heterodimerization results in both ligand-dependent and -independent coordinated alterations of receptor localization and function. *J Biol Chem* **281**, 38812-38824
31. Rozenfeld, R., Gupta, A., Gagnidze, K., Lim, M. P., Gomes, I., Lee-Ramos, D., Nieto, N., and Devi, L. A. (2011) AT1R-CB(1)R heteromerization reveals a new mechanism for the pathogenic properties of angiotensin II. *EMBO J* **30**, 2350-2363
32. Kargl, J., Balenga, N., Parzmair, G. P., Brown, A. J., Heinemann, A., and Waldhoer, M. (2012) The cannabinoid receptor CB1 modulates the signaling properties of the lysophosphatidylinositol receptor GPR55. *J Biol Chem* **287**, 44234-44248
33. Pertwee, R. G. (2009) Emerging strategies for exploiting cannabinoid receptor agonists as medicines. *Br J Pharmacol* **156**, 397-411
34. Whyte, L. S., Ryberg, E., Sims, N. A., Ridge, S. A., Mackie, K., Greasley, P. J., Ross, R. A., and Rogers, M. J. (2009) The putative cannabinoid receptor GPR55 affects osteoclast function in vitro and bone mass in vivo. *Proc Natl Acad Sci U S A* **106**, 16511-16516
35. Rempel, V., Volz, N., Glaser, F., Nieger, M., Brase, S., and Muller, C. E. (2013) Antagonists for the orphan G-protein-coupled receptor GPR55 based on a coumarin scaffold. *J Med Chem* **56**, 4798-4810
36. Moreira, F. A., and Wotjak, C. T. (2010) Cannabinoids and anxiety. *Curr Top Behav Neurosci* **2**, 429-450
37. Sanudo-Pena, M. C., Romero, J., Seale, G. E., Fernandez-Ruiz, J. J., and Walker, J. M. (2000) Activational role of cannabinoids on movement. *Eur J Pharmacol* **391**, 269-274
38. Sulcova, E., Mechoulam, R., and Fride, E. (1998) Biphasic effects of anandamide. *Pharmacol Biochem Behav* **59**, 347-352

FOOTNOTES

*This work was supported by grants from the Spanish Ministry of Economy and Competitiveness (PI11/00295 to CS and a Ramón y Cajal fellowship to PJM) a Madrid Regional Government grant (S2010/BMD-2308 to MG) and funds from the TV3 Marato to PJM (Project 308/C/2013). EP-G is a recipient of Postdoctoral Research Contract from Fundación Científica Asociación Española Contra el Cáncer.

The abbreviations used are: BRET, bioluminescence resonance energy transfer; CB_1R, type-1 cannabinoid receptors; CB_2R, type-2 cannabinoid receptors; CTX, cholera toxin; DMR, dynamic mass

Downloaded from http://www.jbc.org/ by guest on July 18, 2014

redistribution; FK, forskolin; GPCR, G protein-coupled receptors; HBA, 4-[4-(3-hydroxyphenyl)-3-(4-methylphenyl)-6-oxo-1H,4H,5H,6H-pyrrolo[3,4-c]pyrazol-5-yl] benzoic acid; LPI, lysophosphatidylinositol; PLA, proximity ligation assays; PTX, pertussis toxin; THC, Δ^9-tetrahydrocannabinol.

Downloaded from http://www.jbc.org/ by guest on July 18, 2014

FIGURE LEGENDS

FIGURE 1. Expression and functional characterization of CB_2R-GPR55 heteromers in transfected HEK293 cells. A, BRET saturation experiments were performed in cells transfected with a fixed amount of GPR55-Rluc cDNA (0.5 μg) and increasing amounts (1 μg to 5 μg) of CB_2R-YFP or Ghrelin 1a receptor-YFP cDNAs. Values are the mean ± SEM. of 3 to 6 different experiments grouped as a function of the amount of BRET acceptor. B-J, Dynamic mass redistribution (DMR) in HEK-CB_2 (B, C), HEK-GPR55 (D, E) or HEK-CB_2-GPR55 (F-I) cells not treated (B, D, F, G) or treated overnight with 10 ng/mL pertussis toxin (PTX) or with 100 ng/mL cholera toxin (CTX) prior to the addition of the antagonists HBA (B, G) or AM630 (D, F) and stimulation with LPI or HU-308. The resulting picometer-shifts of reflected light wavelength (pm) *vs* time were monitored. Each curve is the mean of a representative optical trace experiment carried out in triplicates.

FIGURE 2. cAMP signaling in HEK293 cells expressing single receptors or CB_2R-GPR55 heteromers. cAMP production in HEK-CB_2 (A-C), HEK-GPR55 (D, E) or HEK-CB_2-GPR55 cells (F, G) treated (B-E, G) or not (A, F) overnight with 10 ng/mL pertussis toxin (PTX) or with 100 ng/mL cholera toxin (CTX). Cells were pre-incubated with vehicle or with the antagonists AM630 or HBA and stimulated with increasing concentrations of HU-308 or LPI in the absence or in the presence of 0.5 μM forskolin (FK). Values are mean ± SEM of n=4-7 and are expressed as a % of the FK-treated cells in each condition. One-way ANOVA followed by Bonferroni post hoc test showed a significant effect over vehicle-treated cells (*$p < 0.05$, **$p < 0.01$, ***$p < 0.001$) or over FK effect ($^{\#\#}p < 0.01$, $^{\#\#\#}p < 0.001$).

FIGURE 3. ERK-1/2 phosphorylation in HEK293 cells expressing single receptors or CB_2R-GPR55 heteromers. A and B, ERK-1/2 phosphorylation was determined in HEK-CB_2 (black bars) or HEK-GPR55 (white bars) cells stimulated with 0.1 μM HU-308 or 1μM LPI for different times (A) or for 7 min with increasing concentrations of HU-308 or LPI (B). In (C-E), ERK-1/2 phosphorylation was determined in HEK-CB_2-GPR55 cells stimulated with 0.1 μM HU-308 or 1μM LPI for different times (C), with increasing concentrations of these compounds for 7 min (D) or in cells pre-treated with vehicle (white bars), with HBA (grey bars) or AM630 (black bars) prior to stimulation with HU-308, LPI or both (E). Phosphorylation was expressed in arbitrary units (ALPHA counts, light emission at 520-620 nm). Values are mean ± SEM of n=6-9 and are expressed as a % over vehicle-treated cells. One-way ANOVA followed by Bonferroni post hoc test showed a significant effect over vehicle-treated cells (*$p < 0.05$, **$p < 0.01$, ***$p < 0.001$) or of the antagonist plus agonist over the agonist treatment (E, ##$p < 0.01$, ###$p < 0.001$).

FIGURE 4. Expression and functional characterization of CB_2R-GPR55 heteromers in BT474 human breast cancer cells. A, BRET saturation experiments were performed in BT474 cells transfected with 1μg of GPR55-Rluc cDNA and increasing amounts of CB_2R-YFP cDNA (1 μg to 3 μg). Values are given as the mean ± SEM of 3 to 7 different experiments grouped as a function of the amount of BRET acceptor. B, A representative result of an *in situ* Proximity Ligation Assay (PLA) performed in BT474-HA-GPR55 cells (left panel). In the confocal microscopy image (superimposed sections) heteromers appear as red spots. Cell nuclei were stained with DAPI (blue). As negative controls (right small panels), PLA were performed in HEK-GPR55 cells in the presence of anti-HA and anti-CB_2R antibodies or in BT474-GPR55 cells in the absence of the anti-HA (CB_2R) or the anti-CB_2R antibodies (GPR55). Scale bars = 20 μm. C-E, DMR analysis in BT474-HA-GPR55 cells not treated (C) or treated overnight with pertussis toxin (D, PTX, 10 ng/mL) or cholera toxin (E, CTX, 100 ng/mL) prior to pre-incubation with the CB_2R or the GPR55 antagonists (AM630 or HBA, respectively), and challenged with LPI or HU-308. The resulting picometer shifts of reflected light wavelength (pm) *vs* time were monitored. Each curve is the mean of a representative optical trace experiment carried out in triplicates.

Downloaded from http://www.jbc.org/ by guest on July 18, 2014

FIGURE 5. cAMP production and ERK-1/2 phosphorylation mediated by CB_2R-GPR55 heteromers in BT474 cancer cells. A and B, cAMP production in BT474-GPR55 cells was determined in cells not pretreated (A) or overnight pre-treated (B) with 10 ng/mL pertussis toxin (PTX) or with 100 ng/mL cholera toxin (CTX) prior to incubation with the CB_2R antagonists AM630 or SR144528 (SR2) or with the GPR55 antagonist HBA (A), and stimulated with HU-308, LPI or both in the absence or in the presence of 0.5 μM forskolin (FK). Values are mean ± SEM of n=3-9 and are expressed as a % of the FK-treated cells. C–E, ERK-1/2 phosphorylation was determined in BT474-GPR55 cells stimulated (7 min) with increasing concentrations of HU-308 or LPI (C), with 0.1 μM HU-308 or 1μM LPI for different times (D) or pre-treated or not with the CB_2R antagonists AM630 or SR144528 (SR2) or with the GPR55 antagonist HBA prior to stimulation with HU-308, LPI or both (E). Phosphorylation was expressed in arbitrary units (ALPHA counts, light emission at 520-620 nm). Values are mean ± SEM of n=3-9 and are expressed as a % of basal levels found in vehicle-treated cells. One-way ANOVA followed by Bonferroni post hoc test showed a significant effect over vehicle-treated cells (***$p < 0.001$, **$p < 0.01$), over FK-treated cells (A, B, ##$p < 0.01$, ###$p < 0.001$) or antagonist plus agonist over the agonist treatment (E, ###$p < 0.001$).

FIGURE 6. Differential effects of THC in HEK293 cells expressing CB_2R-GPR55 heteromers or the single receptors. A-F, cAMP production in the absence/presence of forskolin (FK) (A, C, E) and ERK-1/2 phosphorylation (B, D, F) in response to increasing concentrations of THC in HEK-CB_2 (A, B) and HEK-CB_2-GPR55 (C-F) cells. E and F, cells were pre-treated with vehicle or the antagonists SR2 or HBA. Phosphorylation was expressed in arbitrary units (ALPHA counts, light emission at 520-620 nm). Values are mean ± SEM of n=5-12 and are expressed as a % of FK-treated cells (A, C, E) or of vehicle-treated cells (B, D, F). One-way ANOVA followed by Dunnett's post hoc test showed a significant effect over the effect of FK (E, #$p < 0.05$, ##$p < 0.01$###$p < 0.001$) or over vehicle-treated cells (F, *$p < 0.05$, **$p < 0.01$). G, Schematic representation of the hypothesized effect of THC on CB_2R-GPR55 heteromers is depicted. At low concentrations, THC acts as a CB_2R agonist promoting signaling. At higher concentrations, THC targets GPR55 acting as an antagonist. Via cross-antagonism through the heteromer, high THC concentrations inhibit CB_2R signaling. H-J, DMR responses (H), ERK-1/2 phosphorylation (I) and GTPγS binding (J) in HEK-GPR55 cells in response to LPI, and in the absence or presence of THC (1μM in J). In H, the resulting picometer shifts of reflected light wavelength (pm) *vs* time were monitored. Each curve is the mean of a representative optical trace experiment carried out in triplicates. In I, phosphorylation was expressed in arbitrary units (ALPHA counts, light emission at 520-620 nm). Values are mean ± SEM of n=4-6 and are expressed as a % relative to the effect of LPI. One-way ANOVA followed by Dunnett's post hoc tests showed a significant (***$p < 0.001$) effect over LPI effect. In J, [^{35}S]GTPγS binding was expressed as percentage over basal and values are mean ± SEM of n=3, each one run in triplicates.

FIGURE 7. Involvement of CB_2R-GPR55 heteromers in the response of transfected cancer cells to THC. A, Representative results of *in situ* Proximity Ligation Assays (PLA) performed in BT474-HA-GPR55 cells treated (30 min) with high and low THC concentrations. In the confocal microscopy images (superimposed sections) heteromers appear as red spots. **C**ell nuclei were stained with DAPI (blue). Scale bars = 20 μm. B, The effect of THC on FK-induced cAMP production (left panel) and ERK-1/2 phosphorylation (right panel) in BT474-HA-GPR55 cells is shown. In each panel, a cartoon is included depicting the hypothesized THC mechanism of action. C, cAMP production (upper panel) and ERK-1/2 phosphorylation (lower panel) in BT474-GPR55 cells pre-treated with vehicle or the GPR55 antagonist HBA prior to stimulation with THC. In the upper panel, cells were incubated in the absence or the presence of 0.5 μM forskolin. Phosphorylation was expressed in arbitrary units (ALPHA counts, light emission at 520-620 nm). Values are mean ± SEM of n=5-12 and are expressed as a % of FK-treated cells (cAMP determination) or of vehicle-treated cells (ERK-1/2 phosphorylation). One-way ANOVA followed by Dunnett's post hoc test showed a significant effect over the effect of FK (#$p < 0.05$, ##$p < 0.01$) or over vehicle-treated cells (F, *$p < 0.05$, **$p < 0.01$, ***$p < 0.001$).

Downloaded from http://www.jbc.org/ by guest on July 18, 2014

FIGURE 8. Involvement of CB_2R-GPR55 heteromers in the response to THC of cancer cells endogenously expressing CB_2R and GPR55. A, Top panels show representative results of *in situ* Proximity Ligation Assays (PLA) performed in T98G cells treated (30 min) with vehicle, low and high THC concentrations. In the confocal microscopy images (superimposed sections) heteromers appear as red spots**. C**ell nuclei were stained with DAPI (blue). As negative controls (bottom small panels), PLA were performed in T98G cells in the absence of the anti-CB_2R antibody (GPR55) or the anti-GPR55 antibody (CB_2R), or in the presence of anti-GPR55 and anti-CB_2R antibodies in T98G cells in which CB_2R (T98G-shCB_2) or GPR55 (T89G-shGPR55) were silenced. Scale bars = 20 μm. B, FK-induced cAMP production (left panel) and ERK-1/2 phosphorylation (right panel) in T98G cells in response to THC. In each panel, a cartoon is included depicting the hypothesized THC mechanism of action. C, The volume of subcutaneous tumors generated by injection of T98G cells in immune deficient mice was determined. Tumors were treated with a control siRNA (left panel) or a GPR55-selective siRNA (right panel) and animals received the indicated doses of THC or the corresponding vehicle.Tumor growth curves were compared by ANOVA with a post-hoc analysis by the Student–Newman–Keuls' test. D and E**,** Western blot (D) and densitometric analysis (E) of phospho-ERK-1/2 in control siRNA and GPR55-siRNA tumors treated with 15 mg/Kg THC. *$p < 0.05$ vs vehicle-treated animals (C) or cells (E).

Downloaded from http://www.jbc.org/ by guest on July 18, 2014

Figure 1

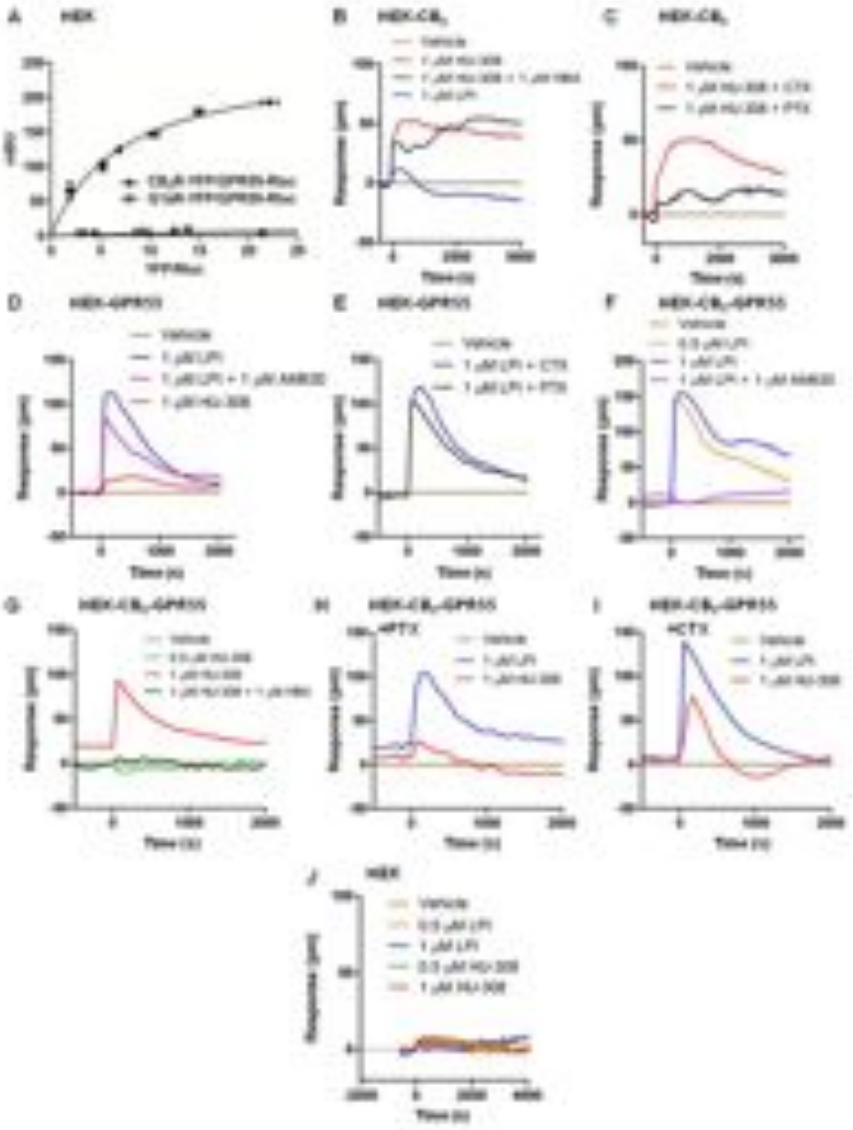

Downloaded from http://www.jbc.org/ by guest on July 18, 2014

Figure 2

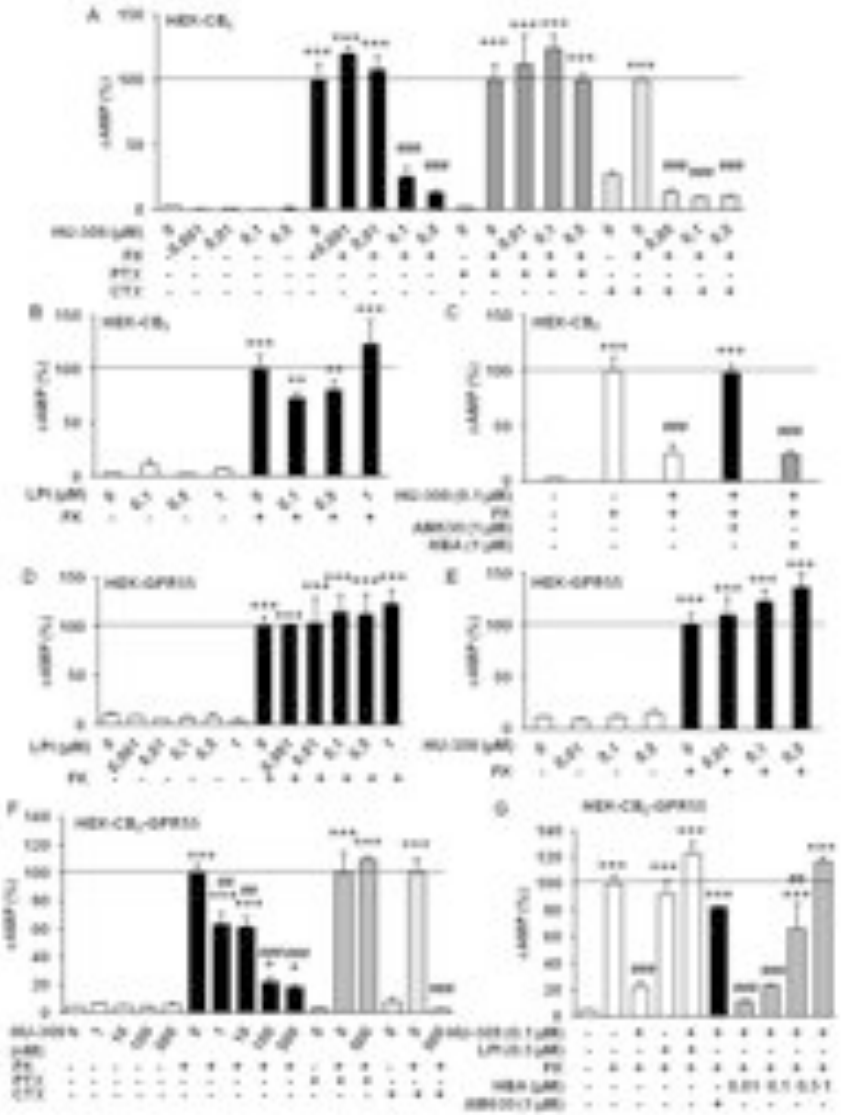

Downloaded from http://www.jbc.org/ by guest on July 18, 2014

Figure 3

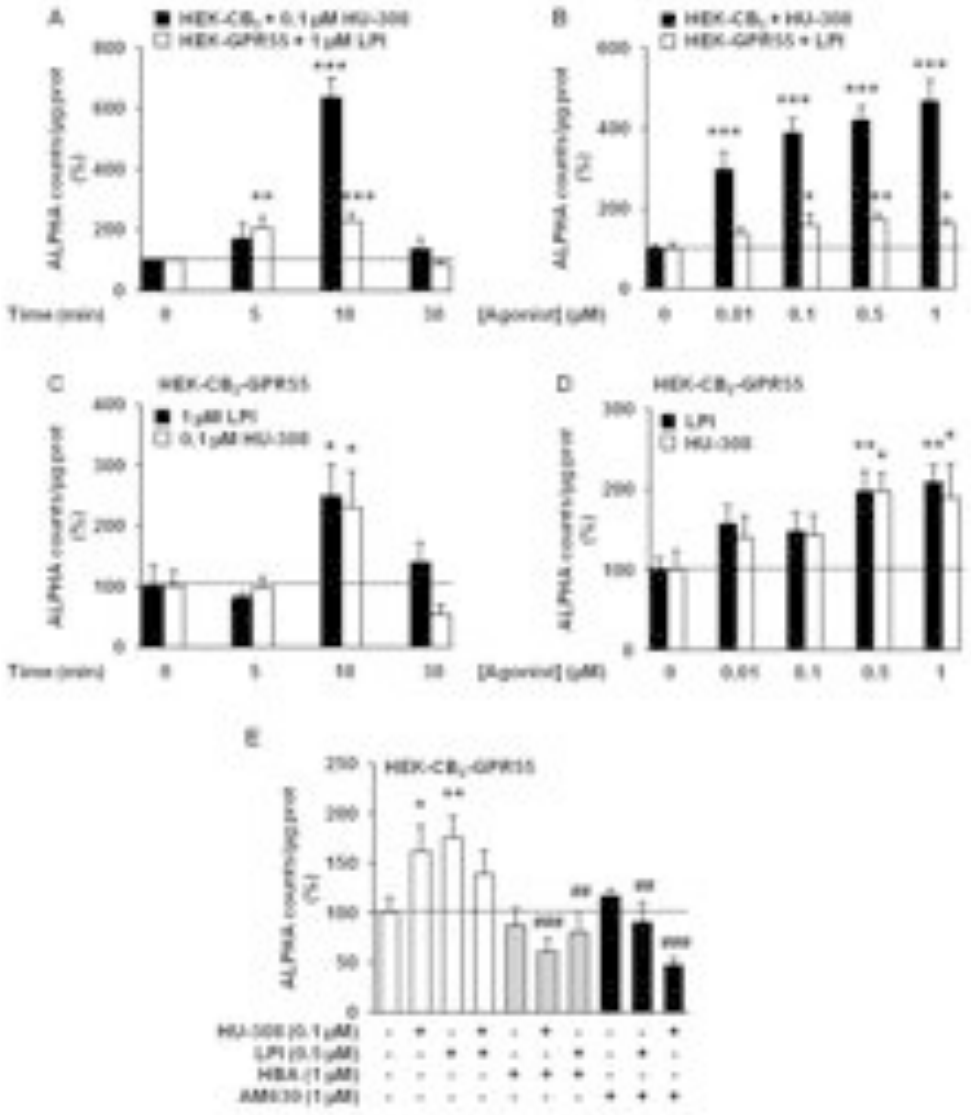

Downloaded from http://www.jbc.org/ by guest on July 18, 2014

Figure 4

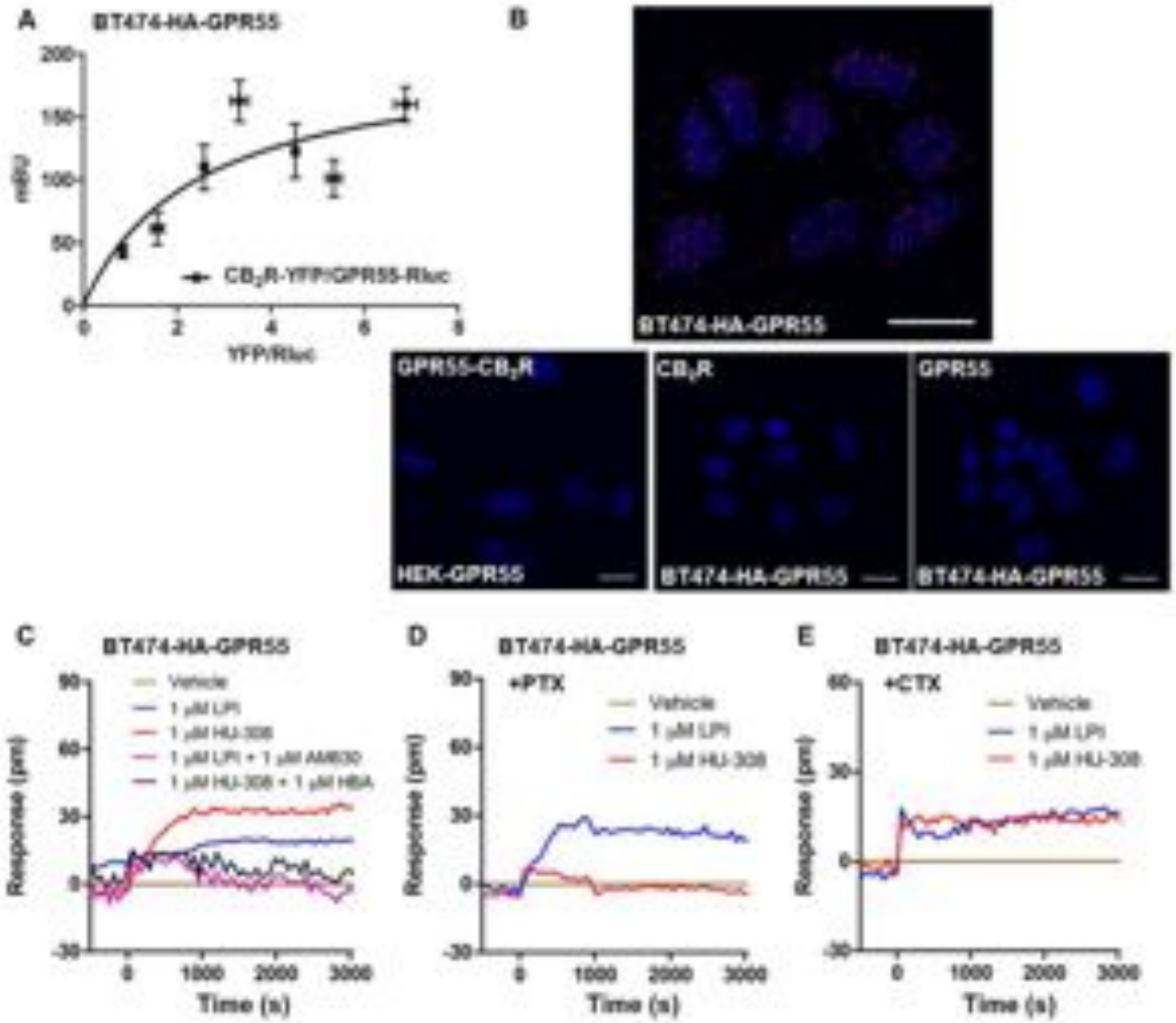

Downloaded from http://www.jbc.org/ by guest on July 18, 2014

Figure 5

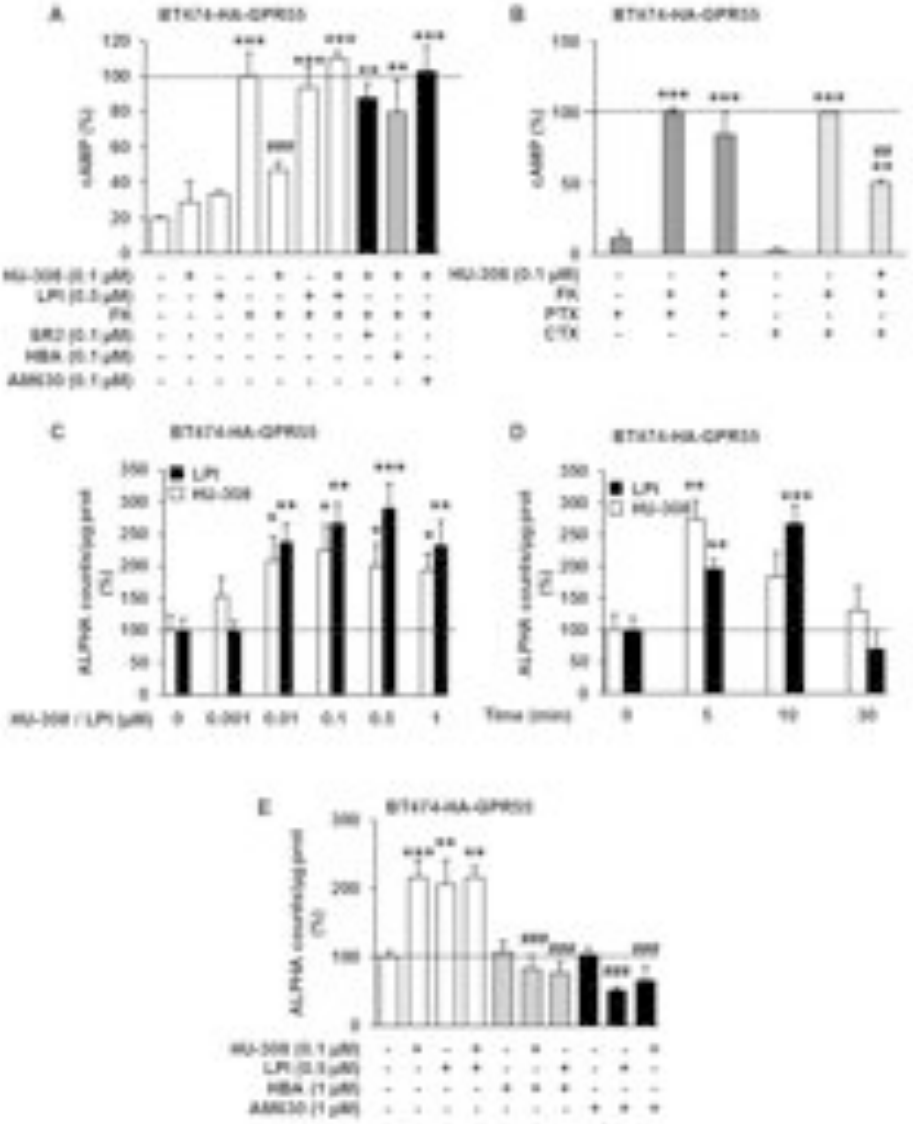

Downloaded from http://www.jbc.org/ by guest on July 18, 2014

Figure 6

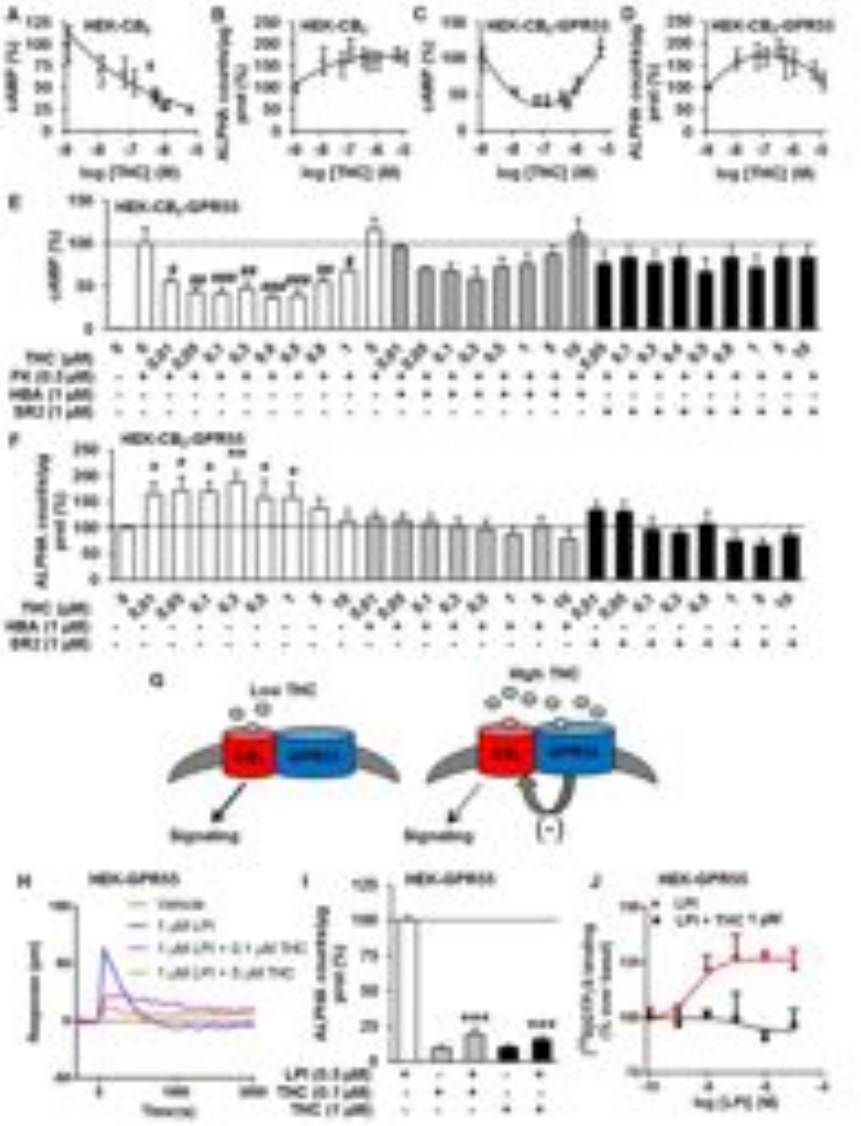

Downloaded from http://www.jbc.org/ by guest on July 18, 2014

Figure 7

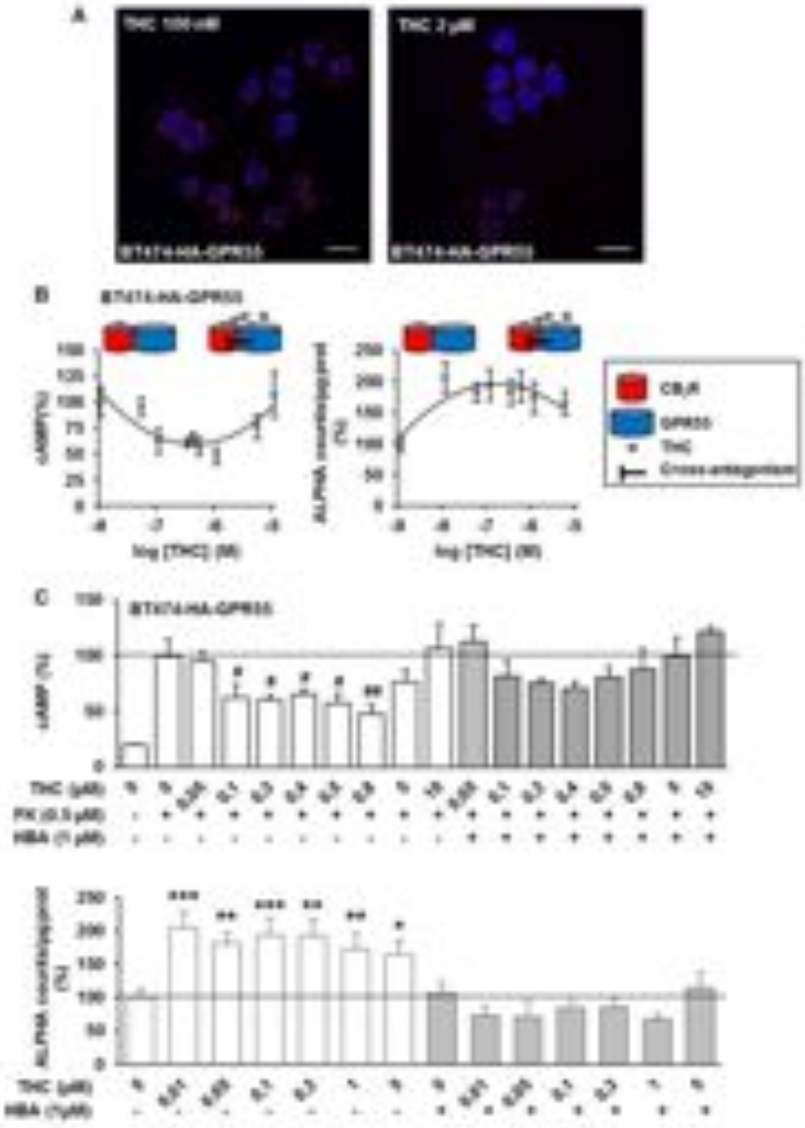

Downloaded from http://www.jbc.org/ by guest on July 18, 2014

Figure 8

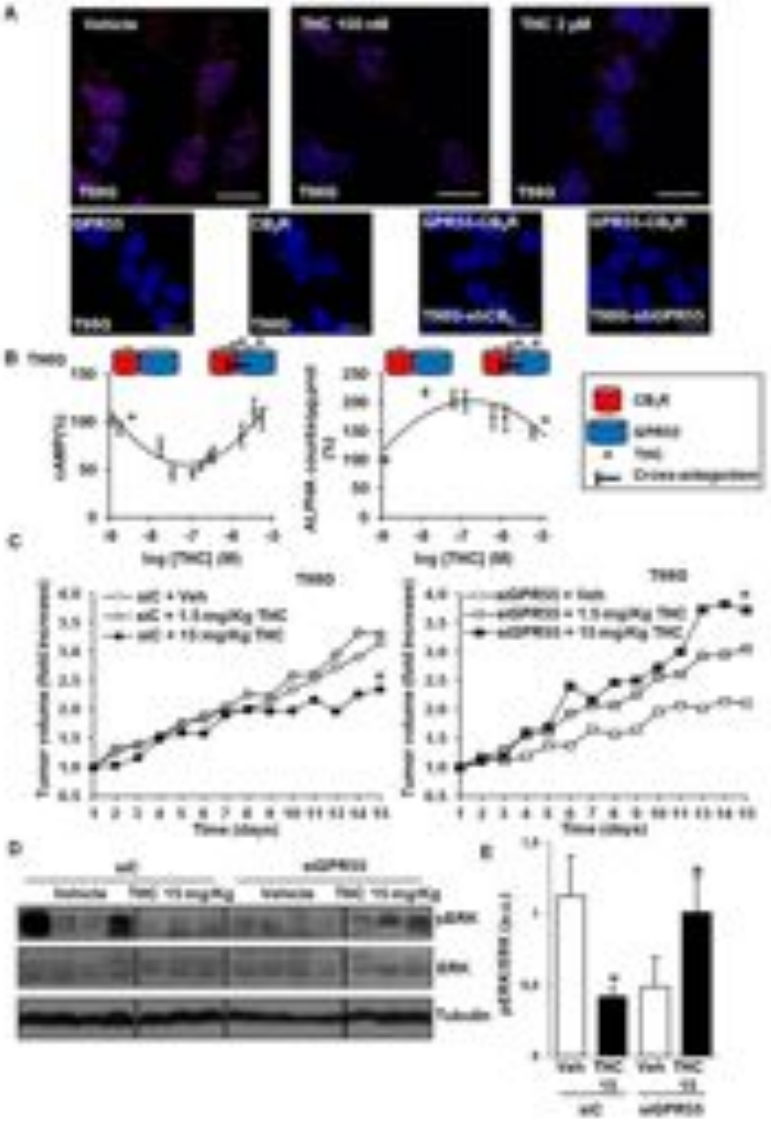

Downloaded from http://www.jbc.org/ by guest on July 18, 2014